ACS chemical biology

Letters

pubs.acs.org/acschemicalbiology

# Diethylaminobenzaldehyde Is a Covalent, Irreversible Inactivator of ALDH7A1

Min Luo,[†] Kent S. Gates,[†] Michael T. Henzl,[‡] and John J. Tanner*[,‡,†]

[†]Department of Chemistry, University of Missouri−Columbia, Columbia, Missouri 65211, United States

[‡]Department of Biochemistry, University of Missouri−Columbia, Columbia, Missouri 65211, United States

Supporting Information

**ABSTRACT:** There is growing interest in aldehyde dehydrogenases (ALDHs) because of their overexpression in cancer stem cells and the ability to mediate resistance to cancer drugs. Here, we report the first crystal structure of an aldehyde dehydrogenase complexed with the inhibitor 4-diethylaminobenzaldehyde (DEAB). Contrary to the widely held belief that DEAB is a reversible inhibitor of ALDHs, we show that DEAB irreversibly inactivates ALDH7A1 via formation of a stable, covalent acyl-enzyme species.

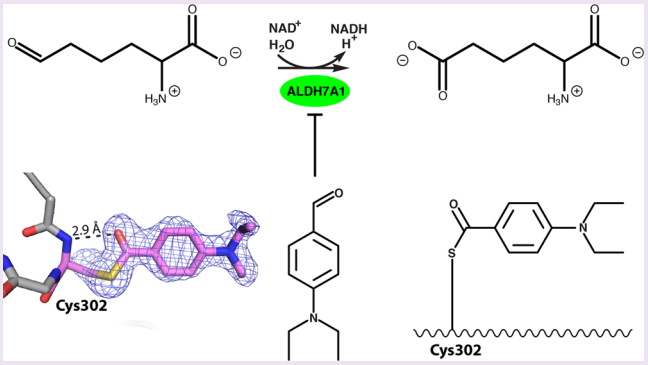


Aldehyde dehydrogenases catalyze the NAD(P)$^+$-dependent oxidation of aldehydes to carboxylic acids. In humans, the aldehyde dehydrogenase (ALDH) superfamily comprises 19 enzymes, which process a diverse array of substrates, including small aldehydes such as acetaldehyde, amino acid derivatives including aminoadipate semialdehyde and glutamate semialdehyde, and large lipids like retinaldehyde and fatty aldehydes such as octanal. ALDHs are important in detoxification of reactive aldehydes, amino acid metabolism, embryogenesis and development, neurotransmission, oxidative stress, and cancer.[1] Consistent with the diversity of substrates and widespread tissue distribution of ALDHs, mutations in ALDH genes are associated with numerous inherited metabolic disorders.[1]

ALDHs have also emerged as important biomarkers of cancer stem cells (CSCs) and mediators of cancer cell resistance to chemotherapeutic agents.[2−5] First discovered in acute myeloid leukemia,[6] CSCs constitute a subpopulation of cells within a heterogeneous tumor and have enhanced tumor-initiating potential because of their ability to regenerate and initiate metastasis. According to the CSC model, conventional cancer therapies reduce tumor mass by killing nontumorigenic cells but leave behind CSCs, resulting in eventual recurrence. The most common method of identifying CSCs is flow cytometry detection of cells expressing high levels of ALDH activity (so-called ALDH bright cells) using fluorescent aldehyde substrates, such as the ALDEFLUOR reagent.[7,8] Overexpression of ALDH1A1, ALDH1A3, ALDH2, ALDH4A1, and ALDH7A1 isoforms has been found in several types of cancers.[9] Because of the functional involvement of ALDHs in CSCs, the correlation between ALDH bright cells and poor clinical outcomes, and the role of ALDHs in cancer drug resistance mechanisms, there is a need for isoform-specific ALDH inhibitors that can be used to probe the various roles of ALDHs in CSCs and as leads in drug development.[5,10]

4-Diethylaminobenzaldehyde (DEAB) is a well-known, but poorly characterized, ALDH inhibitor. DEAB was first identified as an ALDH inhibitor over 25 years ago when the inhibition of ALDH-mediated drug metabolism by DEAB was shown to sensitize cancer cells to the cytotoxic action of cyclophosphamide.[11] More recently, DEAB has been shown to increase the sensitivity of ALDH bright human breast cancer cells to paclitaxel and doxorubicin.[12] DEAB and the related compound 4-dipropylaminobenzaldehyde have been described as reversible competitive inhibitors of ALDH1 (competitive with the aldehyde substrate) with $K_i$ values of 0.04 $\mu$M and 0.01 $\mu$M, respectively.[11,13] Although early work hinted at specificity toward ALDH1A1, more recent studies suggest that DEAB may be a broad inhibitor of ALDHs.[14] Understanding the mechanism and specificity of DEAB is important because DEAB has become an important reagent in cancer research. For example, DEAB is used extensively in cancer drug resistance studies.[5,12,14−16] Furthermore, DEAB is employed as an allegedly ALDH1A1-specific inhibitor in the widely used ALDEFLUOR CSC detection kit.[7] Despite its longstanding and widespread use in medicinal chemistry and cancer biology, the structural basis for the inhibition of ALDH by DEAB has remained unknown.

We herein describe the structural basis of the inhibition of ALDH7A1 by DEAB. ALDH7A1 plays a role in lysine

Received: November 30, 2014
Accepted: January 2, 2015
Published: January 2, 2015

  

DOI: 10.1021/cb500977q
ACS Chem. Biol. 2015, 10, 693−697

catabolism by catalyzing the $NAD^+$-dependent oxidation of $\alpha$-aminoadipate semialdehyde to $\alpha$-aminoadipate. High expression of ALDH7A1 has been found in prostate cancer cell lines, prostate cancer tissue, and matched bone metastasis samples, suggesting that ALDH7A1 plays a functional role in prostate cancer bone metastasis.[17] In addition, patients with ALDH7A1-expressing non-small-cell lung carcinoma tumors have a significantly increased incidence of lung cancer recurrence,[18] and ALDH7A1 expression is increased in ovarian tumors.[19]

Two crystal structures of ALDH7A1 with DEAB bound were determined (Table 1). A 2.4 Å resolution structure having space group *I*422 was determined following cocrystallization of ALDH7A1 with DEAB and a large excess of $NAD^+$ (5 mM). Electron density for $NAD^+$ is strong in the *I*422 form, consistent with the high concentration of $NAD^+$ used in crystallization (Supporting Information Figure S1). A second structure was determined following cocrystallization with DEAB without adding excess $NAD^+$ to the crystallization setup. In this case, 1 mM $NAD^+$ was added to the enzyme during purification, and the enzyme was dialyzed against a buffer devoid of $NAD^+$ prior to crystallization. This protocol produced an *F*222 crystal form that diffracts to 1.95 Å resolution. Electron density for $NAD^+$ is absent in the *F*222 form, which suggests that the final dialysis step reduced the $NAD^+$ concentration to a level that was insufficient to yield high occupancy of the cofactor in this particular crystal form.

ALDH7A1 exhibits the expected ALDH superfamily fold consisting of $NAD^+$-binding, catalytic, and oligomerization domains (Figure 1a). The catalytic domain contains the nucleophilic Cys302 residue that attacks the carbonyl C atom of the aldehyde substrate. The $NAD^+$-binding domain adopts the Rossmann fold. The oligomerization domain mediates

**Table 1. X-ray Diffraction Data Collection and Refinement[a]**

| | DEAB-$NAD^+$ | DEAB |
|---|---|---|
| space group | *I*422 | *F*222 |
| unit cell parameters (Å) | $a = b = 160.3$ | $a = 161.5$ |
| | $c = 320.5$ | $b = 219.4$ |
| | | $c = 233.2$ |
| wavelength | 1.000 | 1.000 |
| resolution (Å) | 59.52−2.40 | 51.49−1.95 |
| | (2.45−2.40) | (1.98−1.95) |
| observations | 606813 | 780650 |
| unique reflections | 81067 | 148899 |
| $R_{merge}(I)$ | 0.144 (0.996) | 0.054 (0.615) |
| $R_{meas}(I)$ | 0.166 (1.146) | 0.068 (0.803) |
| $R_{pim}(I)$ | 0.079 (0.545) | 0.041 (0.510) |
| mean $I/\sigma$ | 12.0 (1.9) | 22.1 (1.8) |
| completeness (%) | 99.7 (95.4) | 99.9 (98.3) |
| multiplicity | 7.5 (7.5) | 5.2 (3.6) |
| no. of protein chains | 4 | 4 |
| no. of protein residues | 2035 | 1933 |
| no. of protein atoms | 15109 | 14441 |
| no. of DEAB atoms | 39 | 39 |
| no. of water molecules | 314 | 516 |
| no. of $NAD^+$ atoms | 176 | n/a |
| $R_{cryst}$ | 0.1803 (0.2532) | 0.1879 (0.2375) |
| $R_{free}$[b] | 0.2348 (0.3057) | 0.2270 (0.2857) |
| RMSD bond lengths (Å) | 0.003 | 0.007 |
| RMSD bond angles (deg) | 0.682 | 0.969 |
| Ramachandran plot[c] | | |
| favored (%) | 96.65 | 98.06 |
| outliers (%) | 0.10 | 0.10 |
| average B-factor (Å$^2$) | | |
| protein | 38.2 | 33.7 |
| DEAB | 39.6 | 42.3 |
| water | 29.9 | 29.8 |
| $NAD^+$ | 32.3 | n/a |
| coordinate error (Å)[d] | 0.29 | 0.20 |
| PDB code | 4X0T | 4X0U |

[a]Values for the outer resolution shell of data are given in parentheses. [b]5% random test set. [c]The Ramachandran plot was generated with RAMPAGE.[26] [d]Maximum likelihood-based coordinate error estimate reported by PHENIX.[27]

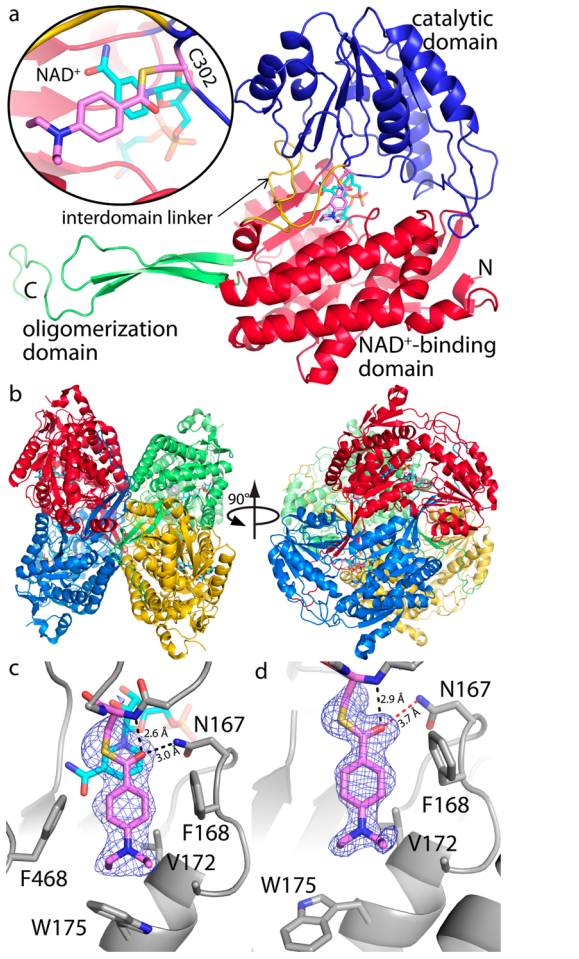


**Figure 1.** Structure of DEAB-inactivated ALDH7A1. (a) Protomer structure, highlighting the domain architecture and DEAB binding site. The three major domains are colored red ($NAD^+$-binding), blue (catalytic), and green (oligomerization). The polypeptide section that links the catalytic and $NAD^+$-binding domains is colored gold. Modified Cys302 and $NAD^+$ are colored pink and cyan, respectively. The inset shows a close-up view of the active site. (b) Two views of the ALDH7A1 tetramer, which is present in both the *I*422 (pictured here) and *F*222 crystal lattices. The four protomers have different colors. Modified Cys302 and $NAD^+$ are colored pink and cyan, respectively. (c) Electron density for covalently modified Cys302 (pink) in the *I*422 crystal form. The mesh represents a simulated annealing $F_o-F_c$ omit map contoured at 2.5$\sigma$. $NAD^+$ is shown in cyan. (d) Electron density for covalently modified Cys302 (pink) in the *F*222 crystal form. The mesh represents a simulated annealing $F_o-F_c$ omit map contoured at 2.5$\sigma$.



DOI: 10.1021/cb500977q
*ACS Chem. Biol.* 2015, 10, 693−697

domain-swapped dimerization. As with certain other ALDHs, two dimers of ALDH7A1 assemble into a tetramer (Figure 1b). We note that this tetramer is present in both crystal lattices reported here as well as the monoclinic lattice reported previously for ALDH7A1.[20] The active site is located in the crevice between the $NAD^+$-binding and catalytic domains, underneath the interdomain linker peptide.

Electron density representing DEAB is evident near the catalytic cysteine, Cys302, in both crystal forms (Figures 1c,d). The maps are consistent with a covalent bond between the S atom of Cys302 and the carbonyl C atom of DEAB. A protruding electron density feature near the S atom indicates the orientation of the C−O bond of DEAB. This feature is more obvious in the higher resolution *F*222 form (Figure 1d). The remaining volume of the density feature is sufficient to accommodate the diethylaminobenzene moiety. This is the first evidence that DEAB forms a stable covalent adduct with an ALDH.

The covalently attached DEAB forms several interactions with the enzyme. We first focus on the *I*422 form (Figure 1c). The O atom of DEAB occupies the oxyanion hole and accepts hydrogen bonds from the main-chain amide of Cys302 and the side chain of Asn167. Whereas one face of the aromatic ring of DEAB packs against the $NAD^+$ nicotinamide and Val172, the other face is highly solvent-accessible. The phenyl ring of DEAB forms edge-to-face $\pi-\pi$ interactions (3.3 Å) with the phenyl rings of Phe168 and Phe468, while the diethylamino moiety sits atop Trp175. These three residues form an aromatic box, which is a conserved feature of ALDH substrate recognition.[21]

Although both structures clearly indicate covalent attachment of DEAB to Cys302, they differ with respect to the local polypeptide conformations and interactions with DEAB. The major difference is that the active site in the *F*222 form is much more open due to conformational disorder of the interdomain linker and the C-terminal 13 residues of the polypeptide chain (Supporting Information Figure S2). Because of this disorder, the interaction of DEAB with aromatic box residue Phe468 is lost in the *F*222 lattice (Figure 1d). Also, Trp175 adopts a different rotamer, which results in less contact with the diethyl groups of DEAB (Figure 1d). Finally, the carbonyl O atom of DEAB forms only one hydrogen bond (with the backbone of Cys302) in the *F*222 form, since the interaction distance with Asn167 is too long for a hydrogen bond (3.7 Å). This difference may be due to the absence of the $NAD^+$ nicotinamide bracing one face of DEAB.

Mass spectrometry was used to confirm the covalent modification seen in the structures. ALDH7A1 was incubated with DEAB and $NAD^+$ prior to analysis with Nano-LC Nanospray QTOF-MS. The spectrum shows a species that has molecular mass of the native enzyme plus 175 Da (Figure 2a). Given a molecular mass of 177 Da for DEAB, the mass spectrum is consistent with a covalent modification having the stoichiometry of one DEAB per protein chain, as observed in the crystal structures.

ALDH activity assays were used to provide further evidence that DEAB is an irreversible inactivator of ALDH7A1. ALDH7A1 was incubated with excess DEAB and $NAD^+$, and the residual ALDH activity was measured as a function of incubation time using hexanal as the substrate. As shown in Figure 2b, DEAB inactivates ALDH7A1 in a time- and concentration-dependent manner. The residual enzyme activity measured as a function of time at five DEAB concentrations

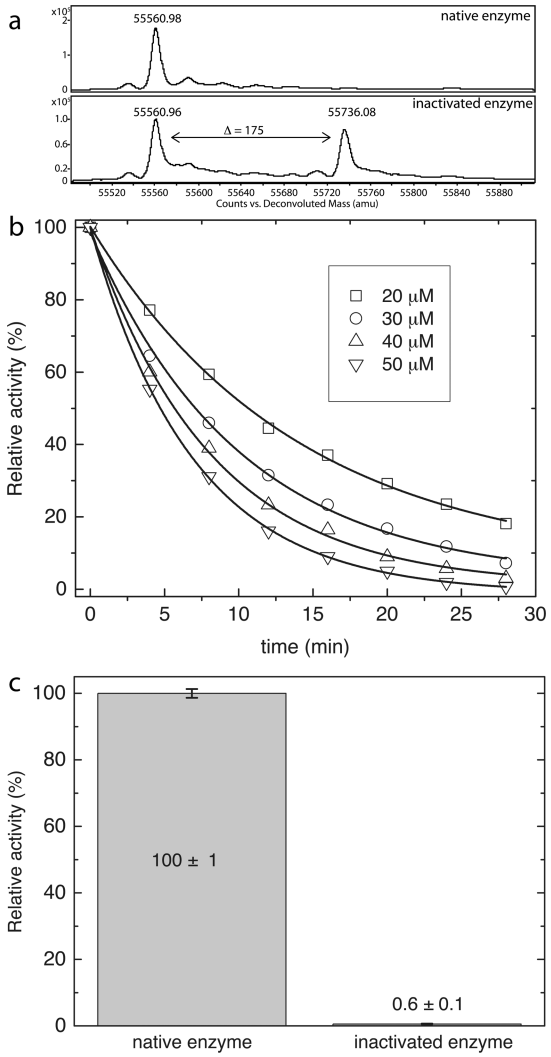


**Figure 2.** Confirmation of covalent inactivation of ALDH7A1 by DEAB. (a) Nano-LC nanospray QTOF mass spectra of native ALDH7A1 (top) and DEAB-inactivated ALDH7A1 (bottom). (b) Residual ALDH activity measured after incubating ALDH7A1 with 20−50 $\mu$M DEAB and 2.5 mM $NAD^+$. (c) ALDH activity measured after gel filtration of native ALDH7A1 (left) and DEAB-inactivated ALDH7A1 (right). The activities are normalized to that of the native enzyme. The error bars were calculated from three trials.

was globally fit to a pseudo-first-order inactivation model (eq 1 of Supporting Information) yielding apparent kinetic parameters of $k_{inact}$ = 0.4 ± 0.1 $min^{-1}$ and $K_I$ = 100 ± 36 $\mu$M. The apparent second-order rate constant for enzyme inactivation by DEAB is $k_{inact}/K_I$ = 70 ± 30 $M^{-1}$ $s^{-1}$. These results are consistent with DEAB being a covalent inactivator of ALDH7A1.

A hallmark of irreversible inactivation is the persistence of inhibition following removal of unbound inhibitor.[22] To investigate this issue, the enzyme (10 $\mu$M) was inactivated by treatment with DEAB (400 $\mu$M) and $NAD^+$ (2.5 mM) and then passed through a size exclusion column to remove excess DEAB. As a control, a sample of ALDH7A1 was treated similarly except that DEAB was omitted. After gel filtration, the DEAB-treated sample exhibited less than 1% of the activity compared to the control (Figure 2c). These results are consistent with covalent, irreversible inactivation of ALDH7A1 by DEAB.



DOI: 10.1021/cb500977q
*ACS Chem. Biol.* 2015, 10, 693−697

Our results contradict the conventional wisdom that DEAB is a noncovalent, reversible inhibitor of ALDHs.[11,13] The notion that DEAB is a reversible inhibitor of ALDHs has always seemed curious, given that DEAB is an aldehyde, and that the related compound, benzaldehyde, is a known substrate for many ALDHs.

Our data indicate that DEAB forms a stable acyl-enzyme species that is a "stalled" intermediate in the enzyme's normal catalytic cycle (Figure 3). In the accepted ALDH mechanism,[10]

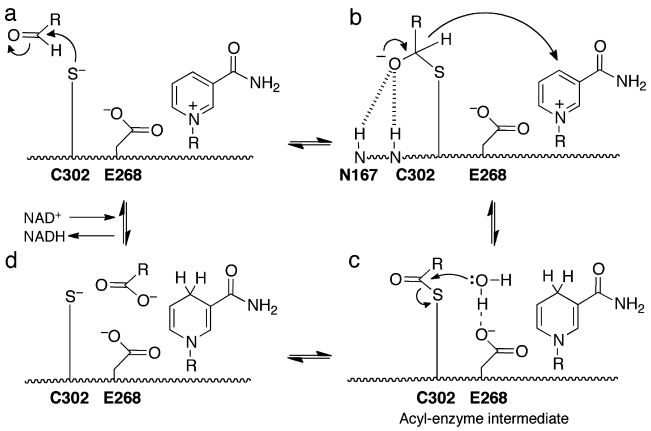


**Figure 3.** Diagram summarizing the accepted mechanism of ALDHs. (a) The aldehyde substrate binds to the active site of the enzyme–$NAD^+$ complex to form a ternary complex. Catalytic Cys302 attacks the carbonyl C atom of the aldehyde substrate. (b) Nucleophilic attack by the catalytic cysteine on the aldehyde produces a hemithioacetal intermediate. Hydrogen bond donors in the oxyanion hole stabilize the negative charge of the hemithioacetal intermediate. (c) Hydride transfer to $NAD^+$ generates NADH and the acyl-enzyme intermediate. Conserved Glu268 activates the water molecule that attacks the acyl-enzyme intermediate. (d) Hydrolysis of the acyl-enzyme intermediate yields the carboxylic acid product, which is released from the enzyme. NADH dissociates and $NAD^+$ binds to regenerate the native enzyme.

nucleophilic attack by the catalytic cysteine on the aldehyde (Figure 3a) produces a hemithioacetal intermediate (Figure 3b). Hydride transfer to $NAD^+$ generates NADH and the acyl-enzyme intermediate (Figure 3c). Hydrolysis of the acyl-enzyme intermediate yields the carboxylic acid product (Figure 3d) and regenerates the native enzyme. The acyl-enzyme intermediate derived from DEAB is apparently stalled. Mass spectral data support the proposed inactivation mechanism. Formation of a stable acyl-enzyme species would be accompanied by the loss of two protons—loss of one to solvent during the activation of Cys302 and transfer of a second, as a hydride ion, from the hemithioacetal to $NAD^+$. Thus, the expected mass-shift for formation of the DEAB acyl-enzyme would be 175 Da, in perfect agreement with the observed mass-shift, measured by mass spectrometry.

The mechanism-based inactivation of SARS main proteinase by benzotriazole esters provides a precedent for the proposed mechanism of inactivation of ALDH7A1 by DEAB.[23,24] In particular, reaction of the proteinase with 1-(4-dimethylamino-benzoyloxy)-benzotriazole results in acylation of the catalytic Cys with 1-(4-dimethylaminobenzoyloxy) (PDB code 2V6N), which is very similar to the covalent adduct that we observe. Donation of electrons from the amino substituent toward the dimethylaminobenzoyloxy thioester is thought to render the adduct resistant to hydrolysis.[23,24] Analogous electronic effects may be at work in our case and may help explain why DEAB is an inactivator of ALDH7A1, whereas benzaldehyde is a substrate.[20]

Alternatively, or at the same time, interactions of DEAB with active site residues may serve to disable the enzyme's hydrolytic machinery. For example, various interactions of DEAB may force the carbonyl of the acyl-enzyme intermediate out of the ideal stereoelectronic alignment required for reaction with the activated water molecule bound to Glu268 at the enzyme active site.[25] Also, Glu268 itself may not be positioned correctly for activating the attacking water molecule. In the normal catalytic cycle, following hydride transfer, the NMN group of NADH rotates out of the active site, allowing Glu268 to rotate into the nicotinamide site to activate the attacking water molecule. In the *F*222 structure, which does not have $NAD^+$ bound, the side chain of Glu268 is disordered in two chains and in the "out" rotamer in the other two chains.

In summary, the inhibition mechanism of DEAB is much different than previously thought. Whether DEAB similarly inactivates other ALDHs remains to be determined, but such investigations should be pursued, given the widespread use of DEAB in the ALDH and CSC research communities. The discovery that DEAB can be an irreversible, covalent inactivator suggests a new strategy for designing ALDH-targeted drugs and probes.

## ■ ASSOCIATED CONTENT

### Supporting Information

The Supporting Information includes Figures S1 and S2, and the experimental details of protein production, crystallization, structure determination, mass spectral analysis, and enzyme activity measurements. This material is available free of charge via the Internet at http://pubs.acs.org.

### Accession Codes

Coordinates and structure factors have been deposited in the Protein Data Bank under accession codes 4X0T (*I*422 form) and 4X0U (*F*222 form).

## ■ AUTHOR INFORMATION

### Corresponding Author

*Phone: (573) 884-1280. Fax: 573-882-2754. E-mail: tannerjj@missouri.edu.

### Notes

The authors declare no competing financial interest.

## ■ ACKNOWLEDGMENTS

We thank B. DaGue of the University of Missouri Charles W. Gehrke Proteomics Center for performing the mass spectrometry studies and J. Nix of Advanced Light Source beamline 4.2.2 for help with X-ray diffraction data collection and processing. Part of the research was performed at the Advanced Light Source, which is supported by the Director, Office of Science, Office of Basic Energy Sciences, of the U.S. Department of Energy under Contract No. DE-AC02-05CH11231.

## ■ REFERENCES

(1) Vasiliou, V., Thompson, D. C., Smith, C., Fujita, M., and Chen, Y. (2013) Aldehyde dehydrogenases: from eye crystallins to metabolic disease and cancer stem cells. *Chem. Biol. Interact. 202*, 2–10.

(2) Ma, I., and Allan, A. L. (2011) The role of human aldehyde dehydrogenase in normal and cancer stem cells. *Stem. Cell. Rev. 7*, 292–306.



DOI: 10.1021/cb500977q
*ACS Chem. Biol.* 2015, 10, 693–697

(3) Muzio, G., Maggiora, M., Paiuzzi, E., Oraldi, M., and Canuto, R. A. (2012) Aldehyde dehydrogenases and cell proliferation. *Free Radic. Biol. Med. 52*, 735−746.
(4) Abdullah, L. N., and Chow, E. K. (2013) Mechanisms of chemoresistance in cancer stem cells. *Clin. Transl. Med. 2*, 3.
(5) Januchowski, R., Wojtowicz, K., and Zabel, M. (2013) The role of aldehyde dehydrogenase (ALDH) in cancer drug resistance. *Biomed. Pharmacother. 67*, 669−680.
(6) Lapidot, T., Sirard, C., Vormoor, J., Murdoch, B., Hoang, T., Caceres-Cortes, J., Minden, M., Paterson, B., Caligiuri, M. A., and Dick, J. E. (1994) A cell initiating human acute myeloid leukaemia after transplantation into SCID mice. *Nature 367*, 645−648.
(7) Balber, A. E. (2011) Concise review: aldehyde dehydrogenase bright stem and progenitor cell populations from normal tissues: characteristics, activities, and emerging uses in regenerative medicine. *Stem Cells 29*, 570−575.
(8) Minn, I., Wang, H., Mease, R. C., Byun, Y., Yang, X., Wang, J., Leach, S. D., and Pomper, M. G. (2014) A red-shifted fluorescent substrate for aldehyde dehydrogenase. *Nat. Commun. 5*, 3662.
(9) Marcato, P., Dean, C. A., Giacomantonio, C. A., and Lee, P. W. (2011) Aldehyde dehydrogenase: its role as a cancer stem cell marker comes down to the specific isoform. *Cell Cycle 10*, 1378−1384.
(10) Koppaka, V., Thompson, D. C., Chen, Y., Ellermann, M., Nicolaou, K. C., Juvonen, R. O., Petersen, D., Deitrich, R. A., Hurley, T. D., and Vasiliou, V. (2012) Aldehyde dehydrogenase inhibitors: a comprehensive review of the pharmacology, mechanism of action, substrate specificity, and clinical application. *Pharmacol. Rev. 64*, 520−539.
(11) Russo, J. E., Hauguitz, D., and Hilton, J. (1988) Inhibition of mouse cytosolic aldehyde dehydrogenase by 4-(diethylamino)-benzaldehyde. *Biochem. Pharmacol. 37*, 1639−1642.
(12) Croker, A. K., and Allan, A. L. (2012) Inhibition of aldehyde dehydrogenase (ALDH) activity reduces chemotherapy and radiation resistance of stem-like ALDHhiCD44(+) human breast cancer cells. *Breast Cancer Res. Treat. 133*, 75−87.
(13) Russo, J., Chung, S., Contreras, K., Lian, B., Lorenz, J., Stevens, D., and Trousdell, W. (1995) Identification of 4-(N,N-dipropylamino)benzaldehyde as a potent, reversible inhibitor of mouse and human class I aldehyde dehydrogenase. *Biochem. Pharmacol. 50*, 399−406.
(14) Moreb, J. S., Ucar, D., Han, S., Amory, J. K., Goldstein, A. S., Ostmark, B., and Chang, L. J. (2012) The enzymatic activity of human aldehyde dehydrogenases 1A2 and 2 (ALDH1A2 and ALDH2) is detected by Aldefluor, inhibited by diethylaminobenzaldehyde and has significant effects on cell proliferation and drug resistance. *Chem. Biol. Interact. 195*, 52−60.
(15) Moreb, J. S., Maccow, C., Schweder, M., and Hecomovich, J. (2000) Expression of antisense RNA to aldehyde dehydrogenase class-1 sensitizes tumor cells to 4-hydroperoxycyclophosphamide in vitro. *J. Pharmacol. Exp. Ther. 293*, 390−396.
(16) Pappa, A., Brown, D., Koutalos, Y., DeGregori, J., White, C., and Vasiliou, V. (2005) Human aldehyde dehydrogenase 3A1 inhibits proliferation and promotes survival of human corneal epithelial cells. *J. Biol. Chem. 280*, 27998−28006.
(17) van den Hoogen, C., van der Horst, G., Cheung, H., Buijs, J. T., Pelger, R. C., and van der Pluijm, G. (2011) The aldehyde dehydrogenase enzyme 7A1 is functionally involved in prostate cancer bone metastasis. *Clin. Exp. Metastasis 28*, 615−625.
(18) Giacalone, N. J., Den, R. B., Eisenberg, R., Chen, H., Olson, S. J., Massion, P. P., Carbone, D. P., and Lu, B. (2013) ALDH7A1 expression is associated with recurrence in patients with surgically resected non-small-cell lung carcinoma. *Future Oncol. 9*, 737−745.
(19) Saw, Y. T., Yang, J., Ng, S. K., Liu, S., Singh, S., Singh, M., Welch, W. R., Tsuda, H., Fong, W. P., Thompson, D., Vasiliou, V., Berkowitz, R. S., and Ng, S. W. (2012) Characterization of aldehyde dehydrogenase isozymes in ovarian cancer tissues and sphere cultures. *BMC Cancer 12*, 329.
(20) Brocker, C., Lassen, N., Estey, T., Pappa, A., Cantore, M., Orlova, V. V., Chavakis, T., Kavanagh, K. L., Oppermann, U., and Vasiliou, V. (2010) Aldehyde dehydrogenase 7A1 (ALDH7A1) is a novel enzyme involved in cellular defense against hyperosmotic stress. *J. Biol. Chem. 285*, 18452−18463.
(21) Riveros-Rosas, H., Gonzalez-Segura, L., Julian-Sanchez, A., Diaz-Sanchez, A. G., and Munoz-Clares, R. A. (2013) Structural determinants of substrate specificity in aldehyde dehydrogenases. *Chem. Biol. Interact. 202*, 51−61.
(22) Silverman, R. B. (1995) Mechanism-based enzyme inactivators. *Methods Enzymol. 249*, 240−283.
(23) Verschueren, K. H., Pumpor, K., Anemuller, S., Chen, S., Mesters, J. R., and Hilgenfeld, R. (2008) A structural view of the inactivation of the SARS coronavirus main proteinase by benzotriazole esters. *Chem. Biol. 15*, 597−606.
(24) Wu, C. Y., King, K. Y., Kuo, C. J., Fang, J. M., Wu, Y. T., Ho, M. Y., Liao, C. L., Shie, J. J., Liang, P. H., and Wong, C. H. (2006) Stable benzotriazole esters as mechanism-based inactivators of the severe acute respiratory syndrome 3CL protease. *Chem. Biol. 13*, 261−268.
(25) Bürgi, H. B., Dunitz, J. D., Lehn, J. M., and Wipff, G. (1974) Stereochemistry of reaction paths at carbonyl centres. *Tetrahedron 30*, 1563−1572.
(26) Lovell, S. C., Davis, I. W., Arendall, W. B., 3rd, de Bakker, P. I., Word, J. M., Prisant, M. G., Richardson, J. S., and Richardson, D. C. (2003) Structure validation by Calpha geometry: phi,psi and Cbeta deviation. *Proteins 50*, 437−450.
(27) Adams, P. D., Afonine, P. V., Bunkoczi, G., Chen, V. B., Davis, I. W., Echols, N., Headd, J. J., Hung, L. W., Kapral, G. J., Grosse-Kunstleve, R. W., McCoy, A. J., Moriarty, N. W., Oeffner, R., Read, R. J., Richardson, D. C., Richardson, J. S., Terwilliger, T. C., and Zwart, P. H. (2010) PHENIX: a comprehensive Python-based system for macromolecular structure solution. *Acta Crystallogr., Sect. D: Biol. Crystallogr. 66*, 213−221.


DOI: 10.1021/cb500977q
*ACS Chem. Biol.* 2015, 10, 693−697